

# Atomic spin-orbit coupling synthesized with magnetic-field-gradient pulses

Zhi-Fang Xu,<sup>1</sup> Li You,<sup>2</sup> and Masahito Ueda<sup>1</sup>

<sup>1</sup>*Department of Physics, University of Tokyo, 7-3-1 Hongo, Bunkyo-ku, Tokyo 113-0033, Japan*

<sup>2</sup>*State Key Laboratory of Low Dimensional Quantum Physics,  
Department of Physics, Tsinghua University, Beijing 100084, China*

(Dated: November 2, 2018)

We discuss a general scheme for creating atomic spin-orbit coupling (SOC) such as the Rashba or Dresselhaus types using magnetic-field-gradient pulses. In contrast to conventional schemes based on adiabatic center-of-mass motion with atomic internal states restricted to a dressed-state subspace, our scheme works for the complete subspace of a hyperfine-spin manifold by utilizing the coupling between the atomic magnetic moment and external magnetic fields. A spatially dependent pulsed magnetic field acts as an internal-state-dependent impulse, thereby coupling the atomic internal spin with its orbital center-of-mass motion, as in the Einstein-de Haas effect. This effective coupling can be dynamically manipulated to synthesize SOC of any type (Rashba, Dresselhaus, or any linear combination thereof). Our scheme can be realized with most experimental setups of ultracold atoms and is especially suited for atoms with zero nuclear spins.

PACS numbers: 03.75.Mn, 67.85.Fg, 67.85.Jk

## I. INTRODUCTION

Synthetic gauge fields recently proposed in the field of quantum gases are widely perceived as being capable of significantly expanding the scopes and possibilities of quantum simulations in condensed matter systems [1]. A U(1) abelian gauge field for neutral atoms allows for exploration of many-body physics such as fractional quantum Hall effects [2]. It acts on atomic internal states much like a magnetic field acting on a charged particle, and has been realized experimentally in atomic condensates using two Raman lasers [3–5], in an optical lattice using Raman-assisted tunneling [6], and in a driven lattice as well [7]. The group of Spielman [8] made an important first step by realizing a spin-orbit coupling (SOC) in a pseudo spin-1/2 system. Several other groups have also been able to realize the same form of SOC not only for bosons [9, 10] but also for fermions [11, 12].

For a two-dimensional system, one commonly distinguishes between two types of SOC: the Rashba SOC  $p_x F_y - p_y F_x$ , which can be transformed into  $p_x F_x + p_y F_y$  via a spin rotation, and the Dresselhaus SOC  $p_x F_y + p_y F_x$ , where  $p_{x,y}$  are the atomic momenta, while  $F_{x,y}$  are the spin- $F$  matrices. The experiment in Ref. [8] realized a special type of SOC which is an equally weighted sum of the above two types ( $\propto p_x F_y$ ). Even richer physics can be simulated with non-abelian gauge fields of more general forms which create, for example, the triangular, square, and kagome lattice phases [13–19]. While these phases appear as ground states of spinor Bose-Einstein condensates (BECs), they need unequal superpositions of Rashba and Dresselhaus SOC. Moreover, Majorana fermions can be realized in 2D fermi gases [20–22] in more general forms of SOC.

Several theoretical proposals have discussed how either Rashba or Dresselhaus SOC can be implemented in neutral atoms [21, 23–25]. Most of them rely on the idea of adiabatic atomic motion in a subspace spanned by sev-

eral spatial-dependent dressed states which are isolated from other levels [1, 26]. An atom with  $N$  internal states is described by an effective Hamiltonian

$$H = \sum_i \mathbf{P}_i^2 / 2m + \sum_{ij} V_{ij}, \quad (1)$$

where  $\mathbf{P}_i$  is the momentum operator associated with the  $i$ -th internal state and  $V_{ij}$ 's denote the internal states' bare energy ( $i = j$ ) and coupling between them ( $i \neq j$ ). When considering a spatial-dependent unitary transformation for the internal basis states  $|\Psi_i(\mathbf{r})\rangle = \sum_{j=1}^N D_{ij}(\mathbf{r}) |\Phi_j(\mathbf{r})\rangle$ , the Hamiltonian in the new (possibly adiabatic) basis  $|\Phi_i(\mathbf{r})\rangle$  becomes

$$H' = \sum_{ij} (\mathbf{P}_i \delta_{ij} - \mathbf{A}_{ij})^2 / 2m + V'_{ij}, \quad (2)$$

with a gauge potential  $\mathbf{A} \equiv i\hbar D^\dagger(\mathbf{r}) \nabla D(\mathbf{r})$  and  $V' \equiv D^\dagger(\mathbf{r}) V D(\mathbf{r})$ . The unitary transformation is nontrivial if the matrix  $V'$  is approximately block diagonalizable and the residual coupling between blocks can be neglected due to large energy differences among blocks. If one of the blocks is spanned by more than one transformed internal state, non-abelian gauge fields appear. An effective approach to realize SOC is to choose a proper transformation  $D$ . For instance, in the multipod scheme, laser beams arranged in a planar form generate a Rashba-type SOC for both spin-1/2 and spin-1 atoms [23]. The protocol in Ref. [24] cyclically couples several ground or metastable states with lasers to overcome collisional decay encountered in the multipod scheme in which dark states are not the lowest single-particle energy states. Inspired by the work of Lin *et al.* [8], two protocols capable of synthesizing pure Rashba and Dresselhaus SOC have also been proposed: one employs a two-dimensional periodic potential formed with bichromatic laser beams which are retro-reflected along two orthogonal directions

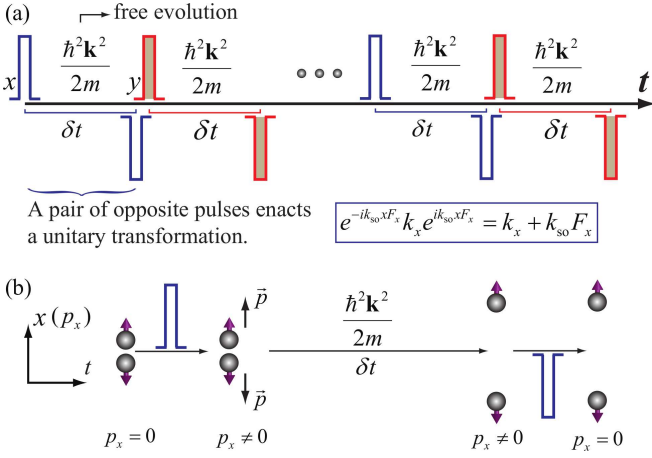


FIG. 1: (Color online). (a) Schematic illustration of creating Rashba SOC in an arbitrary spin- $F$  atom. A pair of opposite magnetic-field pulses causes a spin-dependent momentum change. The pulses along the  $x$ - ( $y$ -) direction are denoted in blue (red-shaded) color. (b) An illustration for the relative displacement and momentum of the spatial wave packets for the two spin states. The spin-dependent impulses lead to a spatial separation of the wave packets upon free evolution as in a beam splitter. The thick arrows inside the shaded dots denote the two spin states.

[21], and the other dynamically generates the two terms of the Rashba SOC in alternate time intervals [25].

Apart from restrictions of their own, none of the above mentioned proposals can be extended to higher spins. In this article, we propose a different approach which synthesizes SOC using space-dependent magnetic field pulses. As we discuss below, our scheme can readily be implemented using the currently available cold atom experimental setups and techniques. It has the potential

to overcome difficulties encountered in previous schemes such as complicated coupling schemes and rather specialized experimental systems. Furthermore, our proposal has the appealing feature of being extendable to higher spins, and it is especially suitable for atoms with zero nuclear spins such as  $^{52}\text{Cr}$  [27],  $^{164}\text{Dy}$  [28], and  $^{168}\text{Er}$  [29], which do not suffer quadratic Zeeman shifts.

## II. PROTOCOL FOR SYNTHESIZING SOC

The SOC we discuss is in general non-abelian; therefore, it cannot be simply gauged away through a unitary transformation [30]. The noncommutativity between two operators, e.g.  $p_x F_x$  and  $p_y F_y$  in a Rashba SOC, is ubiquitous in quantum systems. For instance, in a one-dimensional harmonic trap, the two terms in the Hamiltonian  $H = p_x^2/2m + m\omega^2 x^2/2$  do not commute because  $[x, p_x] = i\hbar$ . Nevertheless, its quantum dynamics can be numerically simulated using the Trotter expansion  $\exp\{-iH\delta t/\hbar\} \simeq \exp\{-i(p_x^2/2m)\delta t/\hbar\} \exp\{-i(m\omega^2 x^2/2)\delta t/\hbar\}$ , to the lowest-order approximation. Alternatively, the inverse process of effecting two noncommuting terms in subsequent time intervals can be adopted to realize an effective dynamics with a Hamiltonian containing noncommuting operators as in the Rashba or Dresselhaus SOC. As long as the two noncommuting terms,  $k_x F_x$  and  $k_y F_y$ , are realized in two different time intervals, simple unitary transformations can be applied to create them by making use of the noncommuting nature between position ( $x, y$ ) and momentum ( $p_x, p_y$ ). Each of the unitary transformation requires two space-dependent magnetic field pulses of opposite signs as illustrated in Figure 1. For a single cycle, the time evolution operator is given by

$$\begin{aligned}
 U(T, 0) &= \left[ U_y(\delta t') e^{-i\frac{\hbar \mathbf{k}^2}{2m} \delta t} U_y^\dagger(\delta t') \right] \times \left[ U_x(\delta t') e^{-i\frac{\hbar \mathbf{k}^2}{2m} \delta t} U_x^\dagger(\delta t') \right] \\
 &= \exp \left\{ -i \frac{\hbar^2}{2m} (k_x^2 + (k_y + k_{so} F_y)^2) \delta t / \hbar \right\} \exp \left\{ -i \frac{\hbar^2}{2m} (k_y^2 + (k_x + k_{so} F_x)^2) \delta t / \hbar \right\} \\
 &\simeq \exp \left\{ -i \left[ \frac{\hbar^2}{2m} (k_x^2 + k_y^2) + \frac{\hbar^2 k_{so}}{2m} (k_x F_x + k_y F_y) + \frac{\hbar^2 k_{so}^2}{4m} (F_x^2 + F_y^2) \right] 2\delta t \right\} \exp(\mathcal{O}(\delta t^2)), \quad (3)
 \end{aligned}$$

where

$$U_\epsilon(\delta t') = \exp\{-iE'_\epsilon \epsilon F_\epsilon \delta t' / \hbar\}, \quad (4)$$

and the leading order error (the second order) is estimated to give

$$\begin{aligned}
 \mathcal{O}(\delta t^2) &= i \frac{\hbar^2 k_{so}^2}{4m^2} \delta t^2 \{ 2k_x k_y F_z + k_{so} k_y (F_x F_z + F_z F_x) \\
 &\quad + k_{so} k_x (F_y F_z + F_z F_y) + i k_{so}^2 [F_y^2, F_x^2] \}. \quad (5)
 \end{aligned}$$

We choose  $\hbar k_{so} \equiv E' \delta t'$  for  $\epsilon = x, y$  by assuming  $E' = E'_x = E'_y$  and  $T = 2\delta t$ , where  $E'_\epsilon$  is proportional to the magnetic field gradient  $B'_\epsilon$ , which is assumed to be strong enough to satisfy the impulse approximation, whereby atomic spatial motion during the short pulse interval  $\delta t'$  ( $\ll \delta t$ ) can be neglected. The validity of our protocol requires the neglect of errors resulting from discrete temporal dynamics from employing the Trotter expansion. We can reasonably estimate the constraint on an energy

cutoff with the leading-order error term  $\mathcal{O}(\delta t^2)$  in Eq. (3) by enforcing  $\hbar^2 k_{\text{so}}^2 \delta t^2 / 4m^2 \times \max(k_{\text{so}} k_\epsilon, k_x k_y, k_\epsilon^2) \ll 1$ . Thus, we realize a Hamiltonian with a Rashba SOC:  $H_R = (p_x^2 + p_y^2) / 2m + \nu(p_x F_x + p_y F_y) + q(F_x^2 + F_y^2)$ , with  $\nu = \hbar k_{\text{so}} / 2m$  and  $q = \hbar^2 k_{\text{so}}^2 / 4m$  denoting respectively the strength of SOC and the quadratic Zeeman shift. More generally, we can realize an arbitrary superposition of the Rashba and Dresselhaus SOC using the same alternating magnetic-field-gradient protocol, but with different pulse durations along the  $x$ - and  $y$ -directions. For instance, we can take  $\delta t_\epsilon = T |v_\epsilon| / \sqrt{v_x^2 + v_y^2}$ , the effective time evolution operator becomes

$$U(T, 0) = U'_y(\delta t') e^{-i \frac{\hbar k^2}{2m} \delta t_x} U'_y{}^\dagger(\delta t') \\ \times U'_x(\delta t') e^{-i \frac{\hbar k^2}{2m} \delta t_y} U'_x{}^\dagger(\delta t'), \quad (6)$$

which gives rise to the an unequal superposition of the Rashba and Dresselhaus SOC  $v_x p_x F_x + v_y p_y F_y$  ( $v_\epsilon > 0$ ), and  $U'_\epsilon \equiv U_\epsilon$ . For  $v_\epsilon < 0$ , everything remains the same except that  $U'_\epsilon \equiv U_\epsilon^\dagger$ .

A static magnetic field must be divergence-free. One thus cannot create a magnetic field with only one-directional spatial gradient. This problem can be circumvented if the other direction with a nonzero gradient is aligned along the  $z$ -axis or the direction perpendicular to the 2D planar system of interest. We further assume that the trapping potential is strongly confined in this direction to suppress the corresponding atomic center-of-mass motion. In actual implementation, one can employ a two-dimensional quadrupole trap (2DQT) [31] in the  $x$ - $z$  plane with  $\vec{B} = B'(x, 0, -z)$  for the first step of each cycle. For the second step, a second 2DQT in the  $y$ - $z$  plane with  $\vec{B} = B'(0, y, -z)$  is required. Although the neglect of quadratic Zeeman shifts causes some error for alkali atoms, such an approximation becomes exact for  $^{52}\text{Cr}$  [27],  $^{164}\text{Dy}$  [28], and  $^{168}\text{Er}$  [29] because their nuclear spins are zero, and hence they have no hyperfine structure.

### III. THE VALIDITY OF OUR PROTOCOL

#### A. Single-atom motion

To demonstrate the validity of our protocol in Eq. (3), we first compare the single-atom motion governed by the effective Rashba-type SOC Hamiltonian  $H_R = (p_x^2 + p_y^2) / 2m + \nu(p_x F_x + p_y F_y) + q(F_x^2 + F_y^2)$  with the actual dynamics of repeated magnetic-field-gradient pulses. The spin-1  $^{87}\text{Rb}$  atom is used as an example. At the semiclassical level, the Heisenberg equations of motion for the Hamiltonian  $H_R$  are described by

$$\frac{d}{dt} \langle x \rangle = \frac{\langle p_x \rangle}{m} + v \langle F_x \rangle, \quad \frac{d}{dt} \langle p_x \rangle = 0, \\ \frac{d}{dt} \langle y \rangle = \frac{\langle p_y \rangle}{m} + v \langle F_y \rangle, \quad \frac{d}{dt} \langle p_y \rangle = 0,$$

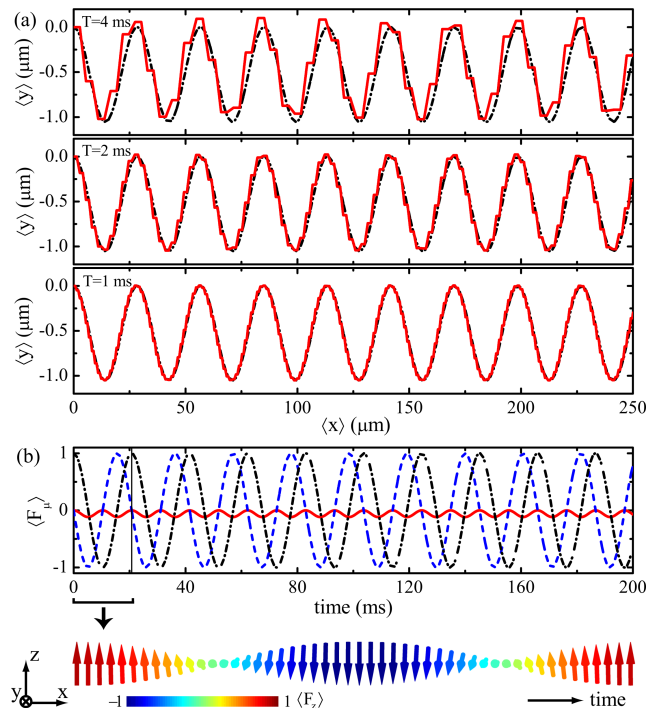


FIG. 2: (color online). (a) Semiclassical trajectories for a spin-1  $^{87}\text{Rb}$  atom in the  $x$ - $y$  plane subjected to an effective Rashba-type SOC (black dot-dashed curves) and to the actual magnetic-field-gradient pulses (red solid curves). From top to bottom,  $T = 2\delta t = 4, 2,$  and  $1$  ms. (b) The corresponding time evolution of averaged spin components  $\langle F_x \rangle$  (red solid curve),  $\langle F_y \rangle$  (blue dashed curve), and  $\langle F_z \rangle$  (black dot-dashed curve) for the semiclassical spatial motion shown in (a) by black dot-dashed curves. The averaged spin vector referenced to the space coordinate frame on the lower left corner is shown in the bottom for a single time period.

$$\frac{d}{dt} \langle F_x \rangle = \frac{v}{\hbar} \langle p_y \rangle \langle F_z \rangle + \frac{q}{\hbar} \left( \langle F_y \rangle \langle F_z \rangle + \langle F_z \rangle \langle F_y \rangle \right), \\ \frac{d}{dt} \langle F_y \rangle = -\frac{v}{\hbar} \langle p_x \rangle \langle F_z \rangle - \frac{q}{\hbar} \left( \langle F_x \rangle \langle F_z \rangle + \langle F_z \rangle \langle F_x \rangle \right), \\ \frac{d}{dt} \langle F_z \rangle = \frac{v}{\hbar} \left( \langle p_x \rangle \langle F_y \rangle - \langle p_y \rangle \langle F_x \rangle \right), \quad (7)$$

where we replace operators by their expectation values, and the correlations among product operators are ignored. Initially the atom is at  $\langle x \rangle = \langle y \rangle = 0$  with its spin fully polarized along the  $z$ -direction, i.e.,  $\langle F_{x,y} \rangle = 0$  and  $\langle F_z \rangle = 1$ ,  $\langle p_y \rangle = 0$ , and  $\langle p_x \rangle^2 / 2mk_B = 0.01$  ( $\mu\text{K}$ ). For a fixed magnetic field pulse area, or  $E' \propto B' \delta t'$ ,  $\delta t'$  can be shortened by increasing  $|B'|$  correspondingly, which further justifies the impulse approximation. According to the Breit-Rabi formula [32], neglecting the quadratic Zeeman shift is quite reasonable in this limit with  $E' = -(5g_I \mu_I + g_J \mu_B) B' / 4$ , where  $g_I$  and  $g_J$  are respectively the Landé factors for the nuclear spin  $\mathbf{I}$  and the electron with total angular momentum  $\mathbf{J}$ ;  $\mu_I$  and  $\mu_B$  are respectively the nuclear magneton and the Bohr magneton. A conservative estimate gives a rather practical magnetic field gradient of  $|B'| = 50$  G/cm. For the pulse

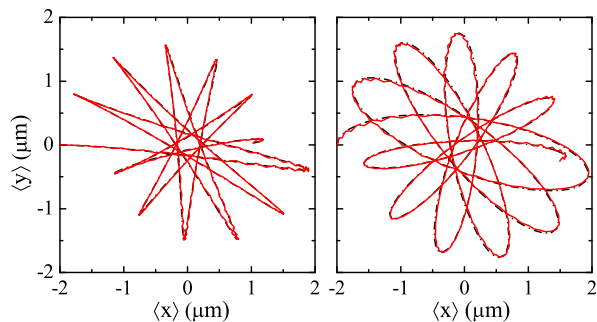


FIG. 3: (color online). Quantum trajectories corresponding to Fig. 2 with  $T = 1$  ms,  $x_0 = -2 \mu\text{m}$ ,  $\omega = 2\pi \times 30$  Hz. The spin state is  $\zeta = (1, 0, 0)^T$  for (a) and  $\zeta = [-i \cos^2(\pi/8), \sin(\pi/4)/\sqrt{2}, i \sin^2(\pi/8)]^T$  for (b). The trajectories obtained from the effective Rashba-type SOC are shown by black dot-dashed curves.

duration, we take  $\delta t' = 0.02$  ms for illustrative purposes. This gives a strength of SOC for spin-1  $^{87}\text{Rb}$  atoms characterized by  $k_{\text{so}} \simeq 2\pi \times (14 \mu\text{m})^{-1}$ , smaller than from the Raman coupling scheme already realized [8].

Figure 2 compares the above effective dynamics with the actual dynamics for a spin-1  $^{87}\text{Rb}$  atom in the  $x$ - $y$  plane with magnetic-field pulses of duration 4, 2, 1 ms from top to bottom. The atomic center-of-mass motion is neglected during the pulses. With sufficiently small  $\delta t$ , the semiclassical dynamics shows that the atomic trajectories are essentially identical to those with an effective Rashba-type SOC. Furthermore, since no trap potential exists in the  $x$ - $y$  plane, the trembling motion observed here is analogous to *Zitterbewegung*, whose presence in ultracold atoms with SOC was proposed in Refs. [33, 34], and the experimental observation was reported in Ref. [35].

Our discussion and derivation above assume a homogeneous system. When an inhomogeneous trapping potential is present, a similar derivation can be carried out as long as the unitary transformations from magnetic-field-gradient pulses commute with local operators. We therefore obtain an effective Hamiltonian  $H'_R = H_R + V(x, y)$ , where  $V(x, y)$  is the trapping potential. We now study the quantum motion of a single atom by numerically solving the corresponding Schrödinger equation. Figure 3 shows the numerically calculated trajectories for a spin-1  $^{87}\text{Rb}$  atom with an initial off-center Gaussian state  $|\psi\rangle = \zeta \exp\{-((x-x_0)^2 + y^2)/2a_{\text{ho}}^2\}/\sqrt{\pi}a_{\text{ho}}$ , where  $V(x, y) = m\omega^2(x^2 + y^2)/2$ ,  $a_{\text{ho}} = \sqrt{\hbar/m\omega}$ , and  $\zeta$  is the spin wave function. We apply the same square magnetic-field-gradient pulses as in Fig. 2, with the period of each cycle chosen to be  $T = 1$  ms.

Different from the homogeneous case, the atomic linear momentum is no longer conserved when a trapping potential is present. In the absence of SOC, an atom initially at rest located at  $(x_0, 0)$  in the  $x$ - $y$  plane will undergo linear oscillations along the  $x$ -axis. With SOC, however, atomic center-of-mass motions in the two or-

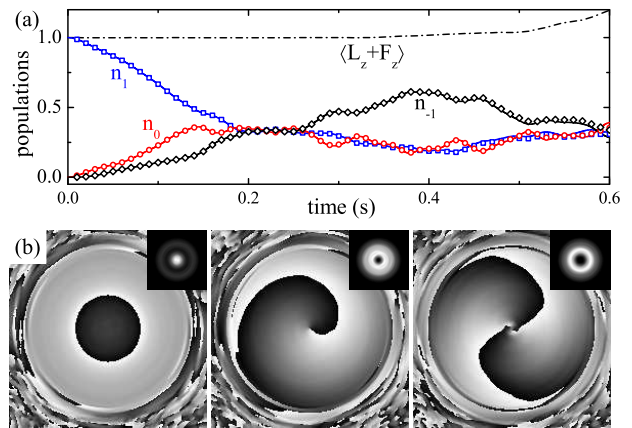


FIG. 4: (color online). (a) Time-dependent population fractions  $n_{M_F} = N_{M_F}/N$  of a spin-1  $^{87}\text{Rb}$  condensate with the atom number  $N_{M_F}$  in the  $M_F$  spin state, with a Rashba-type SOC (solid lines) or the actual magnetic-field-gradient pulses for  $T = 1$  ms and  $B'\delta t' = 1 \text{ G} \cdot \text{ms}/\text{cm}$  (squares, circles, and diamonds for  $M_F = 1, 0, -1$ , respectively, at the end of each 10 periods). The dot-dashed curve shows the time evolution of the sum of the  $z$ -component orbital angular momentum  $L_z$  and the spin component  $F_z$  from the actual dynamics with magnetic-field-gradient pulses at the end of each period. (b) Phase distributions of the three spin states ( $M_F = 1, 0, -1$ , from left to right, respectively) at  $t = 0.2$  s, obtained using Eq. (3). Here, the black (white) color corresponds to the phase  $-\pi$  ( $\pi$ ). The corresponding density distributions over an area of  $30a_{\text{ho}} \times 30a_{\text{ho}}$  are shown in the insets.

thogonal directions are coupled as a result of the non-commuting nature between the two vector gauge potentials. We therefore obtain cyclotron-like motions as shown in Fig. 3, where the actual trajectories depend strongly on the initial spin state.

## B. Dynamics of a condensate

Similar to position-dependent trapping potentials, contact interactions between atoms also commute with the unitary transformations affected by magnetic-field pulses. Therefore, the effective Hamiltonian  $H_R$  can be augmented simply by the trapping potential as well as the interaction terms when a condensate of many atoms is considered. We can then study the analogous dynamics for a spin-1  $^{87}\text{Rb}$  condensate in a pancake potential  $V(x, y, z) = m\omega^2(x^2 + y^2 + \lambda^2 z^2)/2$  with  $\omega = 2\pi \times 30$  Hz and  $\lambda = 100$ , governed by the effective coupled 2D Gross-Pitaevskii equations as in Ref. [36]:

$$\begin{aligned}
 i\hbar \frac{\partial \psi_{\pm 1}}{\partial t} &= \left[ H_0 + H_{\pm 1 \pm 1}^{\text{ZM}} + c_2^{(2\text{D})} (n_{\pm 1} + n_0 - n_{\mp 1}) \right] \psi_{\pm 1} \\
 &\quad + c_2^{(2\text{D})} \psi_{\mp 1}^* \psi_0^2 + H_{\pm 1 0}^{\text{ZM}} \psi_0 + H_{\pm 1 \mp 1}^{\text{ZM}} \psi_{\mp 1}, \\
 i\hbar \frac{\partial \psi_0}{\partial t} &= \left[ H_0 + H_{00}^{\text{ZM}} + c_2^{(2\text{D})} (n_1 + n_{-1}) \right] \psi_0 \\
 &\quad + 2c_2^{(2\text{D})} \psi_0^* \psi_1 \psi_{-1} + H_{01}^{\text{ZM}} \psi_1 + H_{0-1}^{\text{ZM}} \psi_{-1}, \quad (8)
 \end{aligned}$$

where  $H_0 = -\hbar^2 \nabla^2 / 2m + m\omega^2(x^2 + y^2)/2$ ,  $n_i = |\psi_i|^2$ .  $c_{0,2}^{(2D)}$  are effective 2D interaction parameters, and  $H^{ZM}$  is the Zeeman term. We further assume that all atoms are initially populated in the  $M_F = 1$  spin state. In Fig. 4(a), we compare the time-dependent fractional population  $n_{M_F} = N_{M_F}/N$  of the  $M_F$  spin state, with the effective Rashba-type SOC (solid curves) to that obtained from the actual dynamics of the magnetic-field-gradient pulses with  $T = 1$  ms and  $B'\delta t' = 1$  G · ms/cm. From these comparisons, we conclude that the Hamiltonian with an effective SOC well describes the dynamics of the condensate affected by magnetic-field-gradient pulses. The synthesized SOC allows for the realization of the Einstein-de Haas effect: atoms in the  $M_F = 1$  state with a zero angular momentum will be accompanied by vortices with vorticity  $\hbar$  or  $2\hbar$  when transferred to the  $M_F = 0$  or  $-1$  state, while the  $z$ -component of the total angular momentum is conserved. This is clearly demonstrated in Fig. 4. From the dot-dashed curve of Fig. 4(a) we confirm that  $\langle L_z + F_z \rangle$  is almost conserved at the end

of each cycle.

#### IV. AN ALTERNATIVE PROTOCOL

Finally, we consider magnetic fields with both the  $x$ - and  $y$ -dependences. As pointed out in the previous section, SOC of pure Rashba or Dresselhaus types cannot simply be eliminated through unitary transformations. This raises an almost converse question, that is, whether an effective SOC can be created through unitary transformations to a Hamiltonian without SOC. Surprisingly, the answer is yes. We illustrate the following operational protocol with two magnetic field pulses of 2DQT  $\vec{B} = B'(x, -y, 0)$  in the  $x$ - $y$  plane, sandwiched in between the atomic free evolution, like the two oscillating fields in the Ramsey interferometry. The time evolution operator for a spin-1 atom now becomes

$$U(t, 0) = U_{x,y}(\delta t') \exp\left(-i \frac{\hbar^2 \mathbf{k}^2}{2m} t / \hbar\right) U_{x,y}^\dagger(\delta t')$$

$$= \exp\left\{-i \frac{\hbar^2 k_{\text{so}}^2 t}{2m\rho^4 \hbar} \left[ \begin{aligned} &(k_x \rho^2 / k_{\text{so}} + [x^2 + y^2 \text{sinc}(k_{\text{so}}\rho)] F_x + xy[\text{sinc}(k_{\text{so}}\rho) - 1] F_y + [y(1 - \cos k_{\text{so}}\rho) / k_{\text{so}}] F_z)^2 \\ &+ (k_y \rho^2 / k_{\text{so}} - xy[\text{sinc}(k_{\text{so}}\rho) - 1] F_x - [y^2 + x^2 \text{sinc}(k_{\text{so}}\rho)] F_y - [x(1 - \cos k_{\text{so}}\rho) / k_{\text{so}}] F_z)^2 \end{aligned} \right]\right\} \quad (9)$$

where  $U_{x,y}(\delta t') = \exp[-iE'(xF_x - yF_y)\delta t'/\hbar]$ . We thus find that two magnetic-field-gradient pulses give rise to an effective Hamiltonian containing spatially dependent non-abelian gauge fields. In the limit of weak gauge fields and when  $k_{\text{so}}\rho \rightarrow 0$  ( $\rho = \sqrt{x^2 + y^2}$ ), this Hamiltonian reduces to

$$H_{\text{eff}} = \frac{(p_x - A_x)^2}{2m} + \frac{(p_y - A_y)^2}{2m}, \quad (10)$$

where  $A_x = -\hbar(k_{\text{so}}F_x + k_{\text{so}}^2 y F_z / 2)$  and  $A_y = \hbar(k_{\text{so}}F_y + k_{\text{so}}^2 x F_z / 2)$  involve an effective Dresselhaus-type SOC, giving  $\nabla \times \mathbf{A} \neq 0$ .

In an actual implementation, the magnetic-field pulses do not have to be perfectly rectangular as we show earlier. The more important parameter is the area of a pulse. Therefore, a reasonably smooth temporal profile will be sufficient. The effective impulse from the pulse changes the atomic momentum by  $\int_0^{\delta t'} E' dt$ , where  $E' \propto B'$  should be large enough for us to neglect atomic motion during  $\delta t'$ , yet small enough to neglect effects arising from quadratic Zeeman shifts. The above conditions seem challenging, yet remain within reach of current experimental setups of cold atoms. Although the present discussion on the validity of our effective Hamiltonian containing SOC is at the single-particle or single-mode (condensate) level, every step along the way for our pro-

ocols can be justified more generally for the many-body spinor atom system with contact interactions and in a trapping potential.

#### V. CONCLUSIONS

In conclusion, we present a scheme of realizing an effective pure Rashba or Dresselhaus SOC by using magnetic-field-gradient pulses. Due to the noncommuting property between momentum and position operators, by applying  $x$ - and  $y$ -dependent magnetic-field pulses alternatively, we can create a pure Rashba-type SOC. By monitoring the single atom motion at both the semiclassical and quantum levels, and also the dynamics of a spin-1 condensate, we confirm that our protocols are valid and practical within current experimental technology. The Dresselhaus-type SOC can be realized by applying two pulses from a single 2DQT, where an effective Hamiltonian involving non-abelian gauge fields approximately emulates the Dresselhaus-type SOC in the limit of small pulse areas. Our scheme can help develop more general protocols that synthesize gauge fields of various types. They remain valid for quantum simulation studies with atomic quantum gases in a variety of settings and apply to interacting systems as well, as long as the explicit

atomic interaction commutes with unitary transformations enacted with magnetic-field-gradient pulses.

This work is supported by Grants-in-Aid for Scientific Research (KAKENHI 22340114 and 22103005), a Global COE Program “the Physical Sciences Frontier”, the Photon Frontier Network Program, from MEXT of Japan, NSFC (No. 91121005 and No. 11004116), the research program 2010THZO of Tsinghua University, and MOST 2013CB922000 of the National Key Basic Research Program of China. Z.F.X. acknowledges support from JSPS (Grant No. 2301327).

*Note added:* Our paper was submitted to PRL on 23th Jan, 2013 and transferred to PRA on 29th Apr, 2013. The idea we present: synthesizing spin-orbit coupling by spatially dependent magnetic fields, is similar to that of [37]. While we restrict atomic motions in a quasi 2D  $xy$ -plane, a strong bias along the  $z$ -axis and a fast oscillating magnetic field along the  $x$ - $z$  plane is used in [37]. The sinusoidal magnetic field amplitude modulation replaces the two magnetic gradient pulses, however, the net effect is essentially the same as ours.

- 
- [1] J. Dalibard, F. Gerbier, G. Juzeliūnas, and P. Öhberg, *Rev. Mod. Phys.* **83**, 1523 (2011).
- [2] N. R. Cooper, *Advances in Physics* **57**, 539 (2008).
- [3] K. J. Günter, M. Cheneau, T. Yefsah, S. P. Rath, and J. Dalibard, *Phys. Rev. A* **79**, 011604 (2009)
- [4] Y.-J. Lin *et al.*, *Phys. Rev. Lett.* **102**, 130401 (2009); Y.-J. Lin *et al.*, *Nature (London)* **462**, 628 (2009).
- [5] Z. Fu *et al.*, *Phys. Rev. A* **84**, 043609 (2011).
- [6] M. Aidelsburger *et al.*, *Phys. Rev. Lett.* **107**, 255301 (2011).
- [7] J. Struck *et al.*, *Phys. Rev. Lett.* **108**, 225304 (2012).
- [8] Y.-J. Lin, K. Jiménez-García, and I. B. Spielman, *Nature (London)* **471**, 83 (2011).
- [9] J.-Y. Zhang *et al.*, *Phys. Rev. Lett.* **109**, 115301 (2012).
- [10] C. Qu *et al.*, e-preprint arXiv:1301.0658.
- [11] P. Wang *et al.*, *Phys. Rev. Lett.* **109**, 095301 (2012).
- [12] L. W. Cheuk *et al.*, *Phys. Rev. Lett.* **109**, 095302 (2012).
- [13] Z. F. Xu, R. Lü, and L. You, *Phys. Rev. A* **83**, 053602 (2011).
- [14] T. Kawakami, T. Mizushima, and K. Machida, *Phys. Rev. A* **84**, 011607(R) (2011).
- [15] H. Hu, B. Ramachandhran, H. Pu, and X.-J. Liu, *Phys. Rev. Lett.* **108**, 010402 (2012).
- [16] S. Sinha, R. Nath, and L. Santos, *Phys. Rev. Lett.* **107**, 270401 (2011).
- [17] Z. F. Xu, Y. Kawaguchi, L. You, and M. Ueda, *Phys. Rev. A* **86**, 033628 (2012).
- [18] E. Ruokokoski, J. A. M. Huhtamäki, and M. Möttönen, *Phys. Rev. A* **86**, 051607 (2012).
- [19] Z. F. Xu, S. Kobayashi, and M. Ueda, e-preprint arXiv:1304.4340.
- [20] J. Liu *et al.*, *Phys. Rev. Lett.* **107**, 026405 (2011).
- [21] J. D. Sau *et al.*, *Phys. Rev. B* **83**, 140510(R) (2011).
- [22] X.-J. Liu, L. Jiang, H. Pu, and H. Hu, *Phys. Rev. A* **85**, 021603(R) (2012).
- [23] J. Ruseckas *et al.*, *Phys. Rev. Lett.* **95**, 010404 (2005); G. Juzeliūnas, J. Ruseckas, and J. Dalibard, *Phys. Rev. A* **81**, 053403 (2010).
- [24] D. L. Campbell, G. Juzeliūnas, and I. B. Spielman, *Phys. Rev. A* **84**, 025602 (2011).
- [25] Z. F. Xu and L. You, *Phys. Rev. A* **85**, 043605 (2012).
- [26] F. Wilczek and A. Zee, *Phys. Rev. Lett.* **52**, 2111 (1984).
- [27] A. Griesmaier *et al.*, *Phys. Rev. Lett.* **94**, 160401 (2005).
- [28] M. Lu *et al.*, *Phys. Rev. Lett.* **107**, 190401 (2011).
- [29] K. Aikawa *et al.*, *Phys. Rev. Lett.* **108**, 210401 (2012).
- [30] T.-L. Ho and S. Zhang, *Phys. Rev. Lett.* **107**, 150403 (2011).
- [31] D. E. Pritchard, *Phys. Rev. Lett.* **51**, 1336 (1983).
- [32] G. K. Woodgate, *Elementary Atomic Structure*, Oxford University Press Inc., second edition, 1980.
- [33] J. Y. Vaishnav and C. W. Clark, *Phys. Rev. Lett.* **100**, 153002 (2008).
- [34] M. Merkl *et al.*, *Europhys. Lett.* **83**, 54002 (2008).
- [35] L. J. LeBlanc, M. C. Beeler, K. Jimenez-Garcia, A. R. Perry, S. Sugawa, R. A. Williams, and I. B. Spielman, e-preprint arXiv:1303.0914.
- [36] Z. F. Xu, P. Zhang, R. Lü, and L. You, *Phys. Rev. A* **81**, 053619 (2010).
- [37] B. M. Anderson, I. B. Spielman, G. Juzeliūnas, e-preprint arXiv:1306.2606.